Theory of inhomogeneous environmental gaussian broadening of resonance Raman excitation profiles for polyatomic molecules in solution

ARTICLE *in* JOURNAL OF RAMAN SPECTROSCOPY · JUNE 1989

Impact Factor: 2.67 · DOI: 10.1002/jrs.1250200604

3 AUTHORS, INCLUDING:

Gia G Maisuradze
Cornell University
52 PUBLICATIONS **605** CITATIONS

JOURNAL OF RAMAN SPECTROSCOPY, VOL. 20, 359–365 (1989)

Theory of Inhomogeneous Environmental Gaussian Broadening of Resonance Raman Excitation Profiles for Polyatomic Molecules in Solution*

Merab G. Zakaraya and Gia G. Maisuradze
Institute of Inorganic Chemistry and Electrochemistry of the Georgian Academy of Sciences, Jikiya 7, 380086 Tbilisi, USSR

Jens Ulstrup†
Chemistry Department A, Building 207, Technical University of Denmark, 2800 Lyngby, Denmark

The effect of static inhomogeneous environmental broadening of Raman excitation profiles and Raman peak intensity distribution of solute molecules was investigated. Homogeneous broadening is represented by Lorentzians and inhomogeneous broadening by Gaussians, where the latter reflect distributions in the purely electronic transition. The Raman scattering cross-section is calculated analytically, and by means of recent optical bandshape theory for Voigt profiles it can be recast into rapidly converging and easily tractable series expansions well suited for numerical data fitting. The profile expressions also apply to arbitrary values of the broadening parameters and in these respects improve on several previous approaches to inhomogeneous broadening. Notable outcomes are that the excitation profile takes the form of a series of Franck–Condon modulated Voigt profiles when the broadening parameters are small compared with the vibrational frequencies of the Raman-active modes. In this limit only diagonal terms in the sum over vibrational quantum numbers contribute. When the broadening parameters are not small, non-diagonal terms are important and lead to additional broadening, profile maximum shifts and bandshape distortion.

INTRODUCTION

Ground and excited molecular electronic states are often coupled to surrounding solvent molecular motion. This can strongly affect both single-photon optical absorption and emission spectral bandshapes[2] and the spectral and excitation profiles in resonance Raman scattering.[3–15] Provided that other broadening mechanisms can be ignored or disentangled from the solute–solvent coupling, most important information about this coupling pattern, in addition to molecular structural information, can in turn be extracted from the single- and two-photon absorption, emission, spectral and excitation profiles. The detail with which such information is available rests, however, on the availability of precise approaches to the interpretation of specific experimental spectral data, from which excited-state molecular structures and electronic relaxation, the nature of the vibronic line broadening and the nature of the electronic–vibrational interaction can ultimately be obtained.

Theory and formalism which incorporate solute–solvent coupling in detail and emphasize different aspects (dynamic, stochastic, inhomogeneous broadening, etc.) of the coupling patterns are available for single-photon processes.[2] Electronic–vibrational coupling involving both a set of local molecular high-frequency modes and a broad distribution of 'collective' environmental modes commonly lead to the following broad classification of the absorption and emission spectral features of the combined solute–solvent system, to which Raman excitation profiles are also conveniently referred.

(*a*) A set of discrete, narrow Lorentzian vibronic lines, separated by the vibrational energies of the intramolecular modes emerges in the weak-coupling limit of solute–solvent interaction. The Lorentzian width is determined by the (small) solute–solvent coupling strength. The $0 \rightarrow 0$ transition almost corresponds to the purely electronic transition and is equivalent to the zero-phonon line of impurity centres in crystals.[16] The narrow linewidth also makes the transitions very sensitive to other broadening mechanisms, in particular excited-state finite lifetimes. The overall lineshape is then a convolution of the lineshapes arising from the individual independent line-broadening mechanisms. If these are both Lorentzians, the convolution is still a Lorentzian, the overall width of which is now the sum of the two component widths. If the additional broadening is Gaussian, the convolution is more complicated and can be expressed by a Voigt profile.[9,17–19]

(*b*) A diffuse spectral envelope of Gaussian components where local mode vibrational structure can still be distinguished arises in the strong-coupling limit of solute–solvent interaction. This is representative of

* A preliminary version of this work was presented at a recent conference.[1]

† Author to whom correspondence should be addressed.

0377-0486/89/060359-07 $05.00

Received 17 August 1988
Accepted 30 November 1989

homogeneous broadening in polar solvents and some charge displacement between the ground and excited electronic states. The Gaussian components correspond to individual local mode vibrational energy levels. For a single local mode of frequency ω the Gaussian components are located equidistantly and separated by ω. The intensity distribution of the components is determined by the equilibrium local mode coordinate displacement between the ground and excited states. The Stokes shift of the local mode $0 \rightarrow 0$ transition relative to the purely electronic transition is given by the solvent reorganization free energy, which is one of the fundamental parameters of the theory. This quantity ranges from a few hundred to several thousand wavenumbers, but can reach much higher values for analogous thermal electron transfer processes.[20]

(*c*) When the solute–solvent interaction is sufficiently strong compared with the local mode vibrational energy, a broad, structureless band which incorporates all the individual vibronic components appears. The band can be Gaussian or display 'asymmetric' deviations from a Gaussian. This behaviour is representative, for example, of intervalence transitions in mixed-valence compounds or for charge-transfer transitions in large organic molecules.

The three broad classes thus correspond to increasing order of solute–solvent coupling strength. The details further depend on the electronic charge redistribution, the coupling strength and vibrational frequencies for the intramolecular modes, the excited-state electronic relaxation, the dielectric properties of the solvent, etc.

Environmental Raman bandwidth modulation has been approached by stochastic models,[12,21–33] as static inhomogeneous broadening effects[1–9,24] and by dynamic views of the solvent nuclear motion.[10–15,25] We note that the 'real' initial and final states in the Raman scattering event are both vibrational states in the electronic ground state, while excited electronic states participate 'virtually.' In crucial respects, electronic–vibrational single-photon spectra, however, still reflect the line intensity distribution in both Raman spectra and excitation profiles. In particular, resonance profiles similar to single-photon absorption profiles appear close to resonance. Raman resonance profiles therefore constitute a powerful complement to absorption spectra, and great efforts have been made to provide precise correlations between the two kinds of profiles and conceptual frames for the different physical broadening mechanisms.

Raman spectral and excitation profiles exhibit greater sensitivity than single-photon transitions to broadening mechanisms other than dynamic environmental broadening. These are in particular excited electronic state decay and inhomogeneous broadening. Disentanglement of the broadening mechanisms in electronic–vibrational transitions has therefore come to rest increasingly on Raman and coherent anti-Stokes Raman scattering (CARS) spectroscopy,[26] rather than single-photon spectroscopy. With respect to solute–solvent interactions, Raman excitation profiles are, however, conveniently referred to the same broad classification as for single-photon transitions. In particular, we have recently shown[15] (see also Refs 13 and 27) that in the limit of strong solute–solvent coupling the excited-state decay properties are unimportant and the excitation profile is solely determined by the solvent and local mode coupling. An interesting outcome is that in contrast to single-photon transitions the profile is Gaussian only very close to the maximum and much broader beyond a fraction of a half-width. In the weak-coupling limit the individual Raman peaks are Lorentzians and dominated by the excited-state lifetime. In this limit the overall lineshape is easily distorted by other broadening mechanisms, of which inhomogeneous broadening is particularly important.

Investigation of the effects of these competitive mechanisms in the weak-coupling limit is the subject of this paper. More specifically, we have investigated the Raman excitation profile when two broadening mechanisms operate at the same time in the weak-coupling limit of solute–solvent interaction. One of these is Lorentzian and representative either of finite excited-state lifetimes or of weak solute–solvent coupling. The other is Gaussian and most adequately representative of inhomogeneous environmental broadening.

The effect of two broadening mechanisms has been approached before. Penner and Siebrand[3] and Mortensen[4] considered a distribution of purely electronic level gaps in addition to the homogeneous lifetime broadening. For mathematical convenience they used a Lorentzian distribution of the gap ν_{eg} relative to the average value of this gap, $\bar{\nu}_{eg}$, i.e.

$$\rho(\nu_{eg}) = \sigma/[(\nu_{eg} - \bar{\nu}_{eg})^2 + \sigma^2] \qquad (h = 1) \qquad (1)$$

where $\rho(\nu_{eg})$ is the probability that the gap assumes the particular value ν_{eg} and σ is the inhomogeneous width of the distribution. Inhomogeneous broadening of a Lorentzian absorption band of width Γ_{hom} leads to a broader Lorentzian band, the overall width of which is $\Gamma_{tot} = \Gamma_{hom} + \sigma$. In contrast, in the Raman spectral profiles, Γ_{hom} and σ appear in separate terms.

Samoč *et al.*[8] used a Gaussian level gap distribution

$$\rho(\nu_{eg}) = \frac{1}{\sqrt{2\pi}\sigma} \exp\left[-(\nu_{eg} - \bar{\nu}_{eg})^2/2\sigma^2\right] \qquad (2)$$

for direct experimental data fitting to excitation profiles of β-carotene. This form is a more realistic representation of real, local environmentally induced molecular properties. Mortensen[9] noted the relation of the resulting second-order scattering form to the complex error function. Lukashin and Frank-Kamenetskiĭ[5–7] analysed the bandshape resulting from Eqn (2) in greater detail. Their approach was, however, subject to two limitations. First, it was argued that the dynamics of low-frequency environmental nuclear modes was unimportant and that these modes could be disregarded. On the other hand, low-frequency modes, weakly coupled to the molecular charge distributions, are essential in order to ensure overall process irreversibility.[28] Second, the general expression for the differential scattering cross-section in Refs 5–7 was given a complex form, and practical application of the scattering cross-section terms was feasible only when the scattering process is entirely dominated either by homogeneous excited-state Lorentzian decay or by inhomogeneous Gaussian broadening. Within the weak-coupling limit of solute–solvent interaction, the formalism reported here is subject to neither of these two limitations.

RESONANCE PROFILES FOR GAUSSIAN INHOMOGENEOUS BROADENING

We consider a molecular Raman scattering process close to resonance between the electronic ground (g) and excited (e) states of a solute molecule, induced by incoming light of frequency ν. The intensity profile for a given value of the energy gap ν_{eg}, corresponding to the n_gth excited vibrational state in the electronic ground state, has the form[29]

$$S_{n_g}(\nu) \approx \mu_{eg}^4 \nu\nu'^3 \left| \sum_{k_e} \frac{\langle 0_g|k_e\rangle\langle k_e|n_g\rangle}{\nu - \nu_{eg} - \varepsilon_{k_e} + i\Gamma_{k_e}} \right|^2 \quad (3)$$

$|0_g\rangle$ and $|n_g\rangle$ are the total, many-dimensional vibrational wavefunctions of the vibrational ground and n_gth excited states in the electronic ground state, $|k_e\rangle$ the corresponding wavefunctions in the excited electronic state in resonance with the ground state and ε_{k_e} the vibrational energy of $|k_e\rangle$, counted from the purely electronic transition energy ν_{eg}. In the following we assume that the ground- and excited-state vibrational motion is adequately represented by a set of displaced harmonic oscillators. Finally, μ_{eg} is the electronic dipole matrix element coupling the ground and excited electronic states, ν' the scattered light frequency and Γ_{k_e} the decay constant of the vibronic state $|k_e\rangle$. In Eqn (3) we have omitted several pre-summation factors which represent conversion of the transition probability to the scattering cross-section and which depend weakly on the incoming light frequency.

Equation (3) rests on the following further assumptions specific to the problem being considered:

(*a*) The scattering process is adequately described by the adiabatic and Condon approximations for separation of electronic and nuclear motion. The formalism can be extended to non-Condon effects, for example by means of a Herzberg–Teller scheme.

(*b*) The initial electronic–vibrational state is the ground vibrational state for all nuclear modes involved. The implication of this for the molecular, Raman-active modes is straightforward, namely that the vibrational frequencies are large enough that only Stokes processes need to be considered. On the other hand, the frequency dispersion of the structurally disordered environment extends to the lowest frequencies. Equation (3) therefore essentially implies that the dynamic effect of these modes is small, i.e. Eqn (3) must correspond to the weak-coupling limit of solute–solvent interaction, and the main role of the continuous low-frequency environmental modes is to ensure overall process irreversibility.[28] The opposite limit of strong solute–solvent coupling must incorporate both thermal averaging and intermediate state summation with respect to these modes. This limit has recently been considered in detail elsewhere.[15]

(*c*) The lifetime broadening parameter, Γ_{k_e}, leads to a Lorentzian lineshape for corresponding single-photon absorption. Lorentzian absorption bands also emerge in the weak-coupling limit of solute–solvent interaction, the line broadening here being determined by the coupling features in the low-frequency limit of the solvent dispersion.[30,31] It can be shown that the lifetime broadening and dynamic homogeneous environmental coupling part in the weak-coupling limit appear in an entirely equivalent fashion, giving an overall Lorentzian band the width of which is the sum of the two broadening parameters. Such a calculation is not available for two-photon scattering processes.

Combination of Eqns (2) and (3) gives the following expression for the overall inhomogeneously averaged distribution of Raman spectral lines:

$$\bar{S}_{n_g}(\bar{\nu}) \approx \mu_{eg}^4 \nu\nu'^3 \sum_{k_e, m_e=0}^{\infty} \langle 0_g|k_e\rangle\langle k_e|n_g\rangle\langle 0_g|m_e\rangle \times \langle m_e|n_g\rangle G_{k_e m_e}(\bar{\nu}) \quad (4)$$

where

$$G_{k_e m_e}(\bar{\nu}) = \frac{1}{\sqrt{2\pi}\sigma} \int_{-\infty}^{\infty} \frac{\exp\left[-(\bar{\nu}-\nu)^2/2\sigma^2\right]}{(\nu - \varepsilon_{k_e} - i\Gamma_{k_e})(\nu - \varepsilon_{m_e} + i\Gamma_{m_e})}\, d\nu \quad (5)$$

and $\bar{\nu}$ is the average of the excitation frequency, i.e. the value of ν relative to the average of the distribution of the purely electronic transition, or $\bar{\nu} = \nu - \nu_{eg}$. Equations (4) and (5) are the bandshape expressions which we shall subsequently convert to tractable forms, applicable to experimental bandshape data. First we note, however, two more implications of the view of the broadening mechanisms represented by Eqns (3)–(5):

(*d*) Inhomogeneous environmental broadening is assumed to be reflected solely in the energy gap. As an environmental effect, inhomogeneous broadening is in principle also reflected in Γ_{k_e} and Γ_{m_e}. These represent non-radiative excited-state decay modes which also depend on the energy gap between the given excited vibronic level and the level manifold to which it decays.[32] This energy gap in turn depends on the coupling to the environments.

(*e*) Inhomogeneous broadening implies in a sense that the solute–solvent coupling is strong. In the form of Eqns (3)–(5) this effect is, however, not dynamic, i.e. the solvent configuration distribution is not the equilibrium configuration distribution with respect to the electronic ground- and excited-state charge distributions, but static. Physically this situation is revealed in the clearest fashion by site-selective spectroscopy in frozen solid glasses.[33,34] The individual homogeneous components in Raman excitation profiles can therefore still correspond to the weak-coupling, Lorentzian limit, while the overall bandwidth is large owing to strong, static solute–solvent configurational interactions.

With these reservations, integration of eqn (5) gives

$$G_{k_e m_e}(\bar{\nu}) = i\sqrt{\frac{\pi}{2\sigma^2}} \frac{w(z_{m_e}^*) + w(z_{k_e})}{(\varepsilon_{k_e} - \varepsilon_{m_e}) + i(\Gamma_{k_e} + \Gamma_{m_e})} = \sqrt{\frac{\pi}{2\sigma^2}} \frac{[\phi(\xi_{m_e};\theta_{m_e}) - \phi(\xi_{k_e};\theta_{k_e}) + i(\psi(\xi_{m_e};\theta_{m_e}) + \psi(\xi_{k_e};\theta_{k_e})]}{(\varepsilon_{k_e} - \varepsilon_{m_e}) + i(\Gamma_{k_e} + \Gamma_{m_e})} \quad (6)$$

The dimensionless variables z_s, ξ_s, and θ_s $(s = k_e, m_e)$ are defined as

$$z_s = \xi_s - i\theta_s; \quad \xi_s = \Gamma_s/\sqrt{2}\sigma; \quad \theta_s = (\varepsilon_s - \bar{\nu})/\sqrt{2}\sigma \quad (7)$$

The functions $\psi(\xi_s;\theta_s)$ and $\phi(\xi_s;\theta_s)$ are the real and imaginary part, respectively, of the complex function $w(\xi_s;\theta_s)$:

$$w(\xi_s;\theta_s) = \exp[(\xi_s - i\theta_s)^2][1 - \mathrm{erf}(\xi_s - i\theta_s)] \quad (8)$$

where $\mathrm{erf}(z_s)$ is the probability integral of complex argument,[35] i.e. $\psi(\xi_s;\theta_s) = \mathrm{Re}w(\xi_s;\theta_s)$ and $\phi(\xi_s;\theta_s) = \mathrm{Im}w(\xi_s;\theta_s)$. These functions are tabulated.[36] However, $\psi(\xi_s;\theta_s)$ also coincides with the Voigt profile. Analytical expressions for this profile in the form of rapidly converging and easily tractable series expansions for $\psi(\xi_s;\theta_s)$ and $\phi(\xi_s;\theta_s)$ have recently been derived elsewhere.[18,19] Their explicit forms are

$$\psi(\xi_s;\theta_s) = \exp(-\theta_s^2)\{\exp(\xi_s^2)\cos(2\xi_s\theta_s) \times [1 - \mathrm{cth}(2\pi\xi_s)] + (2\xi_s/\pi)\sum_{n=-\infty}^{\infty}\exp(-\tfrac{1}{4}n^2) \times \mathrm{ch}(n\theta_s)/(n^2 + 4\xi_s^2)\} \quad (9)$$

$$\phi(\xi_s;\theta_s) = \exp(-\theta_s^2)\{\exp(\xi_s^2)\sin(2\xi_s\theta_s) \times [\mathrm{cth}(2\pi\xi_s) - 1] + (1/\pi)\sum_{n=-\infty}^{\infty} n\exp(-\tfrac{1}{4}n^2) \times \mathrm{sh}(n\theta_s)/(n^2 + 4\xi_s^2)\} \quad (10)$$

The Voigt profile covers the whole bandshape variation from a purely Gaussian [$\psi(\xi_s;\theta_s) \to \exp(-\theta_s^2)$ for $\xi_s \to 0$] to a purely Lorentzian form [$\psi(\xi_s;\theta_s) \to \xi_s/\sqrt{\pi}(\xi_s^2 + \theta_s^2)$ for $\xi_s \to \infty$]. Several much simpler interpolation forms of Eqns (9) and (10), valid to great accuracy in different limiting incoming light frequency ranges, were also derived in Refs 18 and 19. These mostly take the form of corrections to Gaussian or Lorentzian dominance close to the band maxima or in the band wings, respectively.

Equations (3)–(10) characterize fully the inhomogeneously broadened Raman excitation profiles and the vibronic peak intensity distribution, and apply to arbitrary values of the two broadening parameters Γ_s and σ. Two limiting profile forms emerge. If the vibrational energies of the active modes, ω_j, significantly exceed both broadening parameters, i.e. if $\omega_j \gg \sigma$ and $\omega_j \gg \Gamma_s$, then the diagonal terms in Eqn (4) dominate by far. This limit is representative for many conjugated π-bond systems (carotenes, porphyrins, etc.) with high-frequency Raman-active modes. By putting $k_e = m_e$ in Eqns (4) and (6) we then obtain the following excitation profile for a single active mode ($\omega_j = \omega$):

$$\bar{S}_{n_g}^{\mathrm{diag}}(\bar{\nu}) \approx \sqrt{\frac{\pi}{2\sigma^2}}\,\mu_{eg}^4\,\nu\nu'^3 \times \sum_{k_e=0}^{\infty}\frac{1}{\Gamma_{k_e}}|\langle 0_g|k_e\rangle\langle k_e|n_g\rangle|^2\psi(\xi_{k_e};\theta_{k_e}) \quad (11)$$

When the active-mode vibrational energy significantly exceeds the broadening parameters, the excitation profile thus assumes the form of a series of Voigt profiles, the peak intensity distribution of which is determined by the local mode Franck–Condon factors and the phenomenological decay parameter of the vibronic level $|k_e\rangle$.

The limit represented by Eqn (11) and the analytical form of this equation greatly facilitate the extraction of both the relaxational and the inhomogeneous broadening parameters from specific excitation profile data. Simple ways of doing this were suggested in Ref. 19. Equation (11) is, however, only valid for small Γ_{k_e}, and when Γ_{k_e} is not significantly smaller than ω, non-diagonal terms in Eqn (4) are important. The following more voluminous, but still analytical form of the excitation profile, including the non-diagonal terms, can be obtained by means of the procedures reported in Refs 18 and 19:

$$\bar{S}_{n_g}^{\mathrm{tot}}(\bar{\nu}) = \bar{S}_{n_g}^{\mathrm{diag}}(\bar{\nu}) + \bar{S}_{n_g}^{\mathrm{non\text{-}diag}}(\bar{\nu}) \quad (12)$$

$\bar{S}_{n_g}^{\mathrm{diag}}(\bar{\nu})$ is given by Eqn (11) and $\bar{S}_{n_g}^{\mathrm{non\text{-}diag}}(\bar{\nu})$ is obtained from Eqn (6). It is apparent from this equation that $G_{k_e m_e}(\bar{\nu}) = G^*_{k_e m_e}(\bar{\nu})$, giving for the sum in eqn (4)

$$\sum_{k_e=0}^{\infty}\sum_{m_e=0}^{\infty}\cdots = 2Re\sum_{k_e=0}^{\infty}\sum_{m_e>k_e}^{\infty}\cdots \quad (13)$$

and consequently for $\bar{S}_{n_g}^{\mathrm{non\text{-}diag}}(\bar{\nu})$

$$\bar{S}_{n_g}^{\mathrm{non\text{-}diag}}(\bar{\nu}) \approx \sqrt{\frac{2\pi}{\sigma^2}}\,\mu_{eg}^4\,\nu\nu'^3 \times \sum_{k_e=0}^{\infty}\sum_{m_e>k_e}^{\infty}\langle 0_g|k_e\rangle\langle k_e|n_g\rangle\langle 0_g|m_e\rangle\langle m_e|n_g\rangle \times \frac{(\Gamma_{m_e} + \Gamma_{k_e})[\psi(\xi_{m_e};\theta_{m_e}) + \psi(\xi_{k_e};\theta_{k_e})] + (\varepsilon_{m_e} - \varepsilon_{k_e})[\phi(\xi_{k_e};\theta_{k_e}) - \phi(\xi_{m_e};\theta_{m_e})]}{(\varepsilon_{m_e} - \varepsilon_{k_e})^2 + (\Gamma_{k_e} + \Gamma_{m_e})^2} \quad (14)$$

where $k_e \neq m_e$.

Equation (14) emphasizes the observation above that the smaller Γ_{k_e} and Γ_{m_e} in comparison with $\varepsilon_{m_e} - \varepsilon_{k_e} = \omega(k_e - m_e)$, the less important is $\bar{S}_{n_g}^{\mathrm{non\text{-}diag}}(\bar{\nu})$ compared with $\bar{S}_{n_g}^{\mathrm{diag}}(\bar{\nu})$.

Equations (11), (12) and (14) constitute the complete bandshape formalism for the inhomogeneously broadened resonance profiles and spectral intensity distributions. These equations can be greatly simplified if all the homogeneous broadening parameters, Γ_s, or correspondingly all values of Γ_{k_e}, take approximately the same value $\Gamma_s \approx \Gamma$. Since Γ_s represents electronic relaxation of the various vibrational substates in the excited electronic state by non-radiative decay channels, they are primarily determined by the energy gap between the excited electronic–vibrational states and the electronic ground state.[29] The assumption of constant Γ_s can therefore be expected to be a reasonable first approximation.

After some algebra, the following explicit form of $\bar{S}_{n_g}^{\mathrm{tot}}(\bar{\nu})$ is obtained for the Raman fundamental, i.e. for

$n_g = 1_g$, from Eqns (11) and (14):*

$$\bar{S}^{\mathrm{tot}}_{n_g=1_g}(\tilde{\nu}) \approx \sqrt{\frac{\pi}{2\sigma^2}}\frac{1}{\Gamma}\mu^4_{eg}\nu\nu'^3 \sum_{k_e=0}^{\infty}\langle 0_g|k_e\rangle\langle k_e|1_g\rangle \times \left\{\psi\left(\xi;\frac{\tilde{\nu}-k_e\omega}{\sqrt{2}\sigma}\right)\sum_{m_e=0}^{\infty}\frac{\langle 0_g|m_e\rangle\langle m_e|1_g\rangle}{1+[(k_e-m_e)\omega/2\Gamma]^2} + \phi\left(\xi;\frac{\tilde{\nu}-k_e\omega}{\sqrt{2}\sigma}\right)\sum_{m_e=0}^{\infty}\langle 0_g|m_e\rangle\langle m_e|1_g\rangle \times \frac{(k_e-m_e)\omega/2\Gamma}{1+[(k_e-m_e)\omega/2\Gamma]^2}\right\} \quad (15)$$

when all $\Gamma_s = \Gamma$. Analogous expressions can be obtained for the overtones. An even compacter form emerges in the limit of small equilibrium coordinate shifts of the Raman active mode, Q_0. This limit was considered by Clark and Dines [37] in calculations of resonance profiles for polynuclear transition metal complexes. For $Q_0 \ll 1$

$$\langle 0_g|0_e\rangle = \langle 1_g|1_e\rangle = 1; \quad \langle 0_g|1_g\rangle = -\langle 1_g|0_e\rangle \doteq -\frac{1}{\sqrt{2}}Q_0 \quad (16)$$

Vibrational quantum numbers higher than unity can be disregarded as the corresponding Franck–Condon factors are vanishingly small for $Q_0 \ll 1$. In this limit the summation in Eqn (3) can therefore be restricted to $k_e = 0$ and 1 and the spectral intensity distributions to the Rayleigh ($n_g = 0$) and fundamental Raman components ($n_g = 1$). Overtones are thus absent in the A-term scattering regime for small displacement, and from Eqns (15) and (16) we obtain

$$\bar{S}^{\mathrm{tot}}_{1_g}(\tilde{\nu}) \approx \sqrt{\frac{\pi}{2\sigma^2}}\frac{1}{\Gamma}\mu^4_{eg}\nu\nu'^3\frac{1}{2}Q_0^2\left[\frac{(\omega/2\Gamma)^2}{1+(\omega/2\Gamma)^2}\right] \times \left\{\psi\left[\xi;\frac{\tilde{\nu}}{\sqrt{2}\sigma}\right)+\psi\left(\xi;\frac{\tilde{\nu}-\omega}{\sqrt{2}\sigma}\right) + \left(\frac{2\Gamma}{\omega}\right)\left[\phi\left(\xi;\frac{\tilde{\nu}}{\sqrt{2}\sigma}\right)-\phi\left(\xi;\frac{\tilde{\nu}-\omega}{\sqrt{2}\sigma}\right)\right]\right\} \quad (17)$$

where ψ and ϕ are given by Eqns (9) and (10), respectively.

Figures 1–4 illustrate the effect of increasing ξ_s, i.e. increasing Γ_s relative to the inhomogeneous broadening parameter σ [cf. Eqn (7)]. The particular model corresponds to a single displaced harmonic local mode of frequency 1500 cm^{-1}, a dimensionless displacement of $Q_0 = 1$, an inhomogeneous Gaussian width of $\sqrt{2}\sigma =$ 300 cm^{-1}, equal values of all the decay parameters Γ_s and scattering into the Raman fundamental $n_g = 1_g$. The figures show in particular:

(1) The non-diagonal terms are indeed insignificant for small ξ_s or Γ_s (Fig. 1).

(2) The non-diagonal terms become increasingly important for larger ξ_s ($\xi_s = 0.5$ and 1, Figs 2 and 3). This leads to both individual line broadening and to shifts of the band maxima approximately proportional to σ.

* Since ω is the circular and ν the linear frequency, a multiplicative factor of $(2\pi)^{-1}$ is implicit in Eqns (15) and (17).

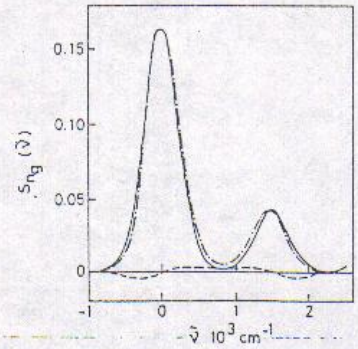

Figure 1. Excitation profile for resonance Raman scattering to the first excited vibrational level ($n_g = 1$) by a single molecular mode of frequency 1500 cm^{-1} and equilibrium coordinate displacement of unity, inhomogeneously broadened by a Gaussian of width $\sqrt{2}\sigma = 300$ cm^{-1}. The plot rests on Eqns (9)–(11) in which the factor in front of the sum with respect to k_e and m_e has been taken as unity. $\xi_s = \Gamma_s/\sqrt{2}\sigma = 0.1$ for all vibronic components ——, Diagonal terms only, - - - -, non-diagonal terms only; · – · –, sum of diagonal and non-diagonal terms.

(3) The non-diagonal terms have different signs in different incoming light frequency regions. The shifts of the zero and first excited band are therefore in opposite directions, the former being blue- and the latter red-shifted. Similar merging towards smaller band separation is caused by 'interference terms' between $0_g \rightarrow 0_e$ and $0_g \rightarrow 1_e$ resonances in wide homogeneously broadened transitions.[37]

(4) For large ξ_s (Fig. 4) the non-diagonal terms have caused the original vibronic bands to coalesce into a single, broad and greatly distorted band in the Raman excitation profile.

Full incorporation of the nondiagonal terms in Eqns (10)–(15) is therefore essential for all but the smallest values of ξ_s or Γ_s.

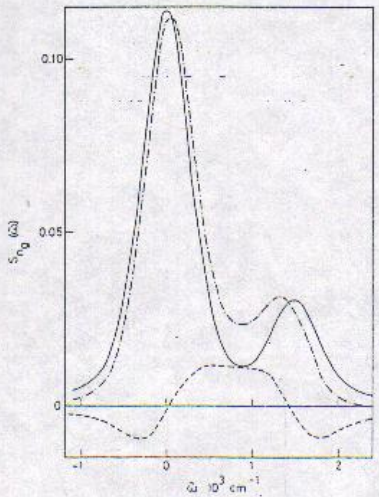

Figure 2. Same profile and parameters as in Fig. 1; $\xi_s = 0.5$ for all components. Lines as in Fig. 1; note the different ordinate scale.

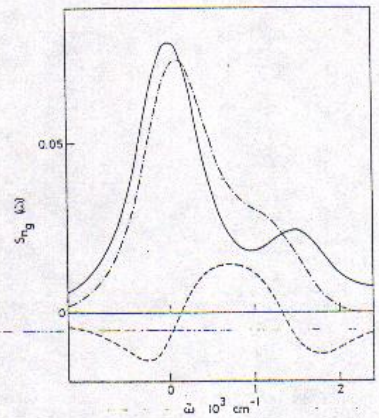

Figure 3. Same profile, parameters and symbols as in Figs 1 and 2; $\xi_s = 1.0$ for all vibronic components.

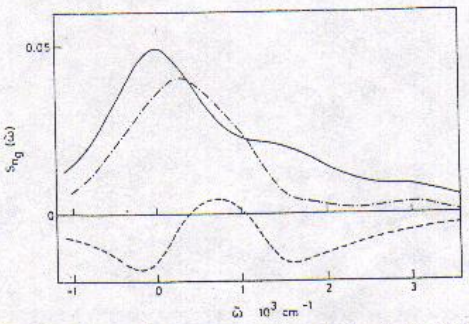

Figure 4. Same profile, parameters and symbols as in Figs 1–3; $\xi_s = 2.0$ for all components. Note different ordinate scale compared with Figs 1–3.

CONCLUSION

Gaussian inhomogeneous environmental broadening, in addition to homogeneous relaxational broadening of the vibronic components in Raman excitation profiles of molecules in solution, leads both to additional broadening and to shifts of individual vibronic peaks. We have provided a formal frame for these effects when the homogeneous broadening is Lorentzian and the environmental broadening Gaussian, the latter representing a distribution with respect to the purely electronic transition. Gaussian broadening is a better representation of real inhomogeneous environmental effects than Lorentzian broadening and in this way improves on previous approaches to environmental effects. Also, although the formalism corresponds to the weak-coupling limit of dynamic solute–solvent interaction, it still extends to all values of both homogeneous and inhomogeneous broadening parameters.

The numerical tractability of our formalism rests on conversion of the Raman scattering cross-section to Voigt profiles. By means of formalism derived elsewhere,[18,19] the integral form of these can be transformed into rapidly converging and easily tractable series, from which the broadening parameters can be obtained by bandshape fitting to specific resonance profile data. In particular, when both relaxational and environmental broadening are small compared with the molecular scattering frequency, the vibronic bands for a given local Raman-active mode take the simplest form, namely a sum over products of single Voigt profiles, local-mode Franck–Condon overlap factors and the inverse broadening parameters. In this limit the individual vibronic bands are symmetrically broadened but insignificantly shifted or distorted. This is because only the diagonal terms in the sum over the local mode vibrational states in the excited intermediate electronic state [Eqn (4)] contribute to the Raman scattering probability. When the broadening parameters are larger, non-diagonal terms in Eqn (4) contribute comparably with the diagonal, Voigt-like terms, leading to broader, more entangled, but still analytical vibronic bandshapes. This formalism should therefore be a convenient tool for extraction of the broadening parameters from specific bandshape data.

Acknowledgements

We thank the Julie Damms Studiefond and the Otto Mønsteds Fond for financial support.

REFERENCES

1. J. Ulstrup and M. G. Zakaraya, in *Proceedings of the XIth International Conference on Raman Spectroscopy*, edited by R. J. H. Clark and D. A. Long, p. 69. Wiley, Chichester (1988).
2. For a recent review, see E. M. Itskovitch, J. Ulstrup and M. A. Vorotyntsev, in *The Chemical Physics of Solvation. Part B. Spectroscopy of Solvation*, edited by R. R. Dogonadze, E. Kálmán, A. A. Kornyshev and J. Ulstrup, p. 223. Elsevier, Amsterdam (1986).
3. A. P. Penner and W. Siebrand, *Chem. Phys. Lett.* **39**, 11 (1976).
4. O. S. Mortensen, *Chem. Phys. Lett.* **43**, 576 (1976).
5. A. V. Lukashin and M. D. Frank-Kamenetskij, *Chem. Phys.* **35**, 469 (1978).
6. A. V. Lukashin, *Opt. Spektrosk.* **52**, 1004 (1982).
7. A. V. Lukashin and M. D. Frank-Mamenetskij, *J. Raman Spectrosc.* **12**, 234 (1982).
8. M. Samoć, W. Siebrand, D. F. Williams, E. G. Woolgar and M. Z. Zgierski, *J. Raman Spectrosc.* **11**, 369 (1981).
9. O. S. Mortensen, *J. Raman Spectrosc.* **11**, 329 (1981).
10. R. A. Desiderio and B. S. Hudson, *Chem. Phys. Lett.* **61**, 445 (1979).
11. K. Kodema and A. D. Bandrauk, *Chem. Phys. Lett.* **80**, 248 (1981).
12. S. Mukamel, *Phys. Rep.* **91**, 1 (1982).
13. G. Delleplane, L. D. Antoni, L. Piseri, L. Staffini and R. Tubino, *J. Phys. Chem.* **88**, 560 (1984).
14. R. R. Dogonadze, T. A. Marsagishvili, M. G. Zakaraya and J.

Ulstrup, in *Proceedings of the International Conference on Electrodynamics and Quantum Phenomena at Interfaces, Metsniereba, Tbilisi, USSR* p. 419, (1986).
15. M. G. Zakaraya and J. Ulstrup, *Chem. Phys.*, in press.
16. K. K. Rebane, *Impurity Spectra of Solids*. Plenum Press, New York (1970).
17. W. Voigt, *S.B. Bayer. Akad. Wiss.*, 603 (1912).
18. M. G. Zakaraya, *Opt. Spektrosk.* **59**, 467 (1985); *Opt. Spectrosc.* (*USSR*) **59**, 282 (1985).
19. M. G. Zakaraya and J. Ulstrup, *Opt. Commun.* **68**, 107 (1988).
20. For a recent review, see A. M. Kuznetsov, J. Ulstrup and M. A. Vorotyntsev, in *The Chemical Physics of Solvation. Part C. Solvation in Specific Physical, Chemical and Biological Systems*, edited by R. R. Dogonadze, E. Kálmán, A. A. Kornyshev and J. Ulstrup, p. 163. Elsevier, Amsterdam (1988).
21. T. Takagahara, E. Hanamura and R. Kubo, *J. Phys. Soc. Jpn.* **43**, 802 (1977).
22. T. Takagahara, E. Hanamura and R. Kubo, *J. Phys. Soc. Jpn.* **43**, 811 (1977).
23. R. Kubo, T. Takagahara and E. Hanamura, *Solid State Commun.* **32**, 1 (1979).
24. M. G. Zakaraya and G. G. Maisuradze, *Opt. Spektrosk.* **63**, 663 (1987); *Opt. Spectrosc.* (*USSR*) **63**, 389 (1987).
25. W. Siebrand and M. Z. Zgierski, *J. Phys. Chem.* **86**, 4718 (1982).
26. See, for example, J. W. Nibler and G. V. Knighten, *Top. Curr. Phys.* **16**, 202 (1979).
27. H. Böttger, V. V. Bryksin and P. Kleinert, *Phys. Status Solidi B* **89**, 675 (1978).
28. E. M. Itskovitch and A. M. Kuznetsov, *Elektrokhimiya* **16**, 755 (1980).
29. A. C. Albrecht, *J. Chem. Phys.* **34**, 1476 (1961).
30. R. R. Dogonadze, A. M. Kuznetsov, M. G. Zakaraya and M. A. Vorotyntsev, *J. Electroanal. Chem.* **75**, 315 (1977).
31. R. R. Dogonadze and M. G. Zakaraya, *Opt. Spektrosk.* **54**, 1019 (1983); *Opt. Spectrosc.* (*USSR*) **54**, 604 (1983).
32. J. Jortner, S. A. Rice and R. M. Hochstrasser, *Adv. Photochem.* **7**, 149 (1969).
33. R. I. Personov, E. I. Al'Shitz, L. A. Bykovskaya and B. M. Kharlamov, *Zh. Eksp. Teor. Fiz.* **65**, 1825 (1973).
34. I. Abram, R. A. Auerbach, R. R. Birge, B. E. Kohler and J. J. Stevenson, *J. Chem. Phys.* **61**, 3857 (1974).
35. M. Abramovitz and I. Stegun, *Handbook of Mathematical Functions*. Dover, New York, 1965.
36. V. N. Faddeeva and N. N. Terent'ev, *Tables of Probability Integrals of Complex Arguments*. Pergamon Press, Oxford (1961).
37. R. J. H. Clark and T. J. Dines, *Mol. Phys.* **42**, 193 (1981).